

1 Catalytic and Non-Catalytic Synergistic Effects and their Individual Contributions to
2 Improved Combustion Performance of Coal/Biomass Blends

3 Jumoke OLADEJO ^a, Stephen ADEGBITE ^b, Hao LIU ^c, Tao WU ^{b,d,*}

4

5 ^a International Doctoral Innovation Centre, The University of Nottingham Ningbo China,
6 Ningbo 315100, China

7 ^b Department of Chemical and Environmental Engineering, The University of Nottingham
8 Ningbo China, Ningbo 315100, China

9 ^c Department of Architecture and Built Environment, The University of Nottingham, University
10 Park, Nottingham NG7 2RD, UK

11 ^d Municipal Key Laboratory of Clean Energy Conversion Technologies, The University of
12 Nottingham Ningbo China, Ningbo 315100, China

13 Corresponding author: tao.wu@nottingham.edu.cn

14

15 **Highlights**

- 16 • Catalytic and non-catalytic synergistic effects on co-firing were distinguished.
17 • The constituents and rank of coal influences the extent of synergy observed.
18 • Non-catalytic synergistic effects are more pronounced in fuel blends.
19 • Synergistic inhibition occurs due to competing synergistic effects.
20 • Individual contribution of catalytic and non-catalytic synergy was quantified

21 **Abstract**

22 This study focuses on the synergistic properties of three types of coal when co-fired
23 with oat straw at different blending ratios. The results demonstrated non-additive
24 interaction between the oat straw and coal samples. The catalytic effect of oat straw

25 ash and the non-catalytic effect of its organic constituents on these coal samples were
26 isolated and analysed to measure their contribution to the confirmed synergistic effects
27 during co-firing. The results showed a level of synergy suppression between catalytic
28 and non-catalytic mechanisms due to the overlap in function of the catalysing alkali
29 and alkaline earth metals (AAEMs) and the hydrogen contributing organic constituents.
30 A novel index, the synergy combination efficiency, was therefore proposed and used
31 to quantify the level of synergistic promotion or synergistic inhibition occurring in the
32 co-firing of these fuel blends. It was found that at a blending ratio of 30 wt% oat straw,
33 the Guizhou coal achieved a synergy factor (S.F) of 1.50, with non-catalytic and
34 catalytic synergy contributing 69.1% and 30.9% respectively. This coal blend had the
35 highest synergistic promotion with combined efficiency of 194%, showing the potential
36 of the use of co-firing synergy to improve the combustion performance of poor quality
37 coals.

38 Keywords – co-firing, catalytic synergy, non-catalytic synergy, synergy index, synergy
39 efficiency

40 List of Abbreviation

AAEMs	Alkali and Alkaline Earth Metals
ATC	Australian Coal
BT	Burnout Temperature
GZC	Guizhou Coal
LRC	Low Rank Coal
LTA	Low Temperature Ash
OS	Oat Straw

OS_LTA	Low Temperature Ash of Oat Straw
OS_WL	Water leached oat straw
S.F	Synergy Factor
S.I	Synergy Index
YNC	Yunnan Coal

41

42 1.0 Introduction

43 Despite the damaging effects of coal usage on the environment, there is a forecasted
44 increase in coal consumption, particular in China, with power generation expected to
45 increase from 900 GW in 2015 to 1775 GW by 2030 [1]. The reserve of China's low
46 rank coal (LRC) is estimated at about 46% of the total proven coal reserves [2]. Most
47 of these LRCs are found in south-western provinces and north-eastern provinces and
48 are considered low grade coals due to the high content of ash, sulphur and/or moisture.
49 Almost three-quarters of China's electricity are generated from coal-fired power plants
50 but the contribution of LRCs to this electricity generation remains inconsequential [3].
51 This is mainly due to several problems associated with the utilization of LRCs such as
52 lower conversion efficiency, higher SO₂ & CO₂ emissions and instances of volatile
53 organic carbons (VOCs) and particulate matter pollution. Recently, there has been an
54 increase in the local utilization of these low rank coals especially in the north-eastern
55 provinces due to their low costs [4, 5]. However, the need to investigate methods of
56 utilising them in more efficient thermal conversion processes is required. Gani,
57 Morishita [6] suggested that the effective large-scale utilisation of LRC would require
58 the improvement of the ignition and burnout performance of the coal by adding
59 supplementary fuels. Hence, co-firing a LRC with biomass can be advantageous due

60 to the higher volatile matter content of biomass which is expected to lead to such
61 improvements. The co-firing of coal with biomass is a simple but cost-effective
62 approach to the large-scale deployment of biomass in pulverized fuel utility boilers.
63 However, owing to the vast difference in the combustion characteristics of biomass
64 and coal, only partial substitution of coal is acceptable in order to reduce the degree
65 of performance incompatibility to an acceptable level [7-9].

66 This partial substitution of coal with biomass offers benefits such as reduced emissions
67 of NO_x, SO_x and greenhouse gases as a result of the low sulphur, low nitrogen and
68 carbon lean nature of biomass compared to coal [10, 11]. This will also improve the
69 economics of biomass utilization as well as its energy conversion efficiency since
70 large-scale fossil-fired plants are more efficient than small-scale biomass plants.
71 Furthermore, partial substitution can improve the efficiency of such power plants with
72 minimal technical risk on implementation [10, 12, 13]. It also allows the usage of a
73 wider range of fuels including low grade coals which are cheaper, hence providing
74 cost incentives.

75 Several studies [8, 14-18] concluded that the ignition temperature, fuel reactivity,
76 burnout and ash deposition behaviour are crucial characteristics for the determination
77 of the suitability of solid fuels for co-firing . However, the results provided by these
78 studies are not always clear due to the conflicting influences of the fuel blends. Some
79 of these studies observed synergistic [19, 20] and/or additive behaviours [20, 21] from
80 fuel blend interactions depicting improvement and/or insignificant change in the
81 performance. Also, the alkali and alkaline earth metals (AAEMs) in biomass were
82 found to enhance coal char reactivity in some cases [22] while differing significantly in
83 others [23].

84 This study focuses on thermal decomposition characteristics of the co-firing of oat
85 straw with different coals and the implications on practical applications. The main
86 interactions between fuels were studied to determine synergetic interactions and to
87 validate the underlying causes.

88 2.0 Material and Methods

89 2.1 Samples

90 Three coal samples (an Australian coal (ATC), a Guizhou coal (GZC) and a Yunnan
91 coal (YNC)) and oat straw (OS) were used for this research. The preparation of
92 samples for experimental study was conducted following the British standard BS EN
93 14780 and ISO 13909 [24, 25]. All the fuel samples were milled using a Retsch SM
94 200 mill (Retsch, Germany) and then sieved to a size of $\leq 106 \mu\text{m}$. Oat straw was
95 blended with the coal samples in two mass fractions, i.e. 10 and 30 wt%. The blending
96 ratio corresponds to the typical co-blending conditions utilised in practice [19].

97 2.2 Fuel Properties

98 2.2.1 Proximate and Ultimate Analysis

99 The proximate analysis was performed using a thermogravimetric analyser (TGA)
100 (STA 449 F3 Netzsch, Germany) using approximately 5–10 mg following the
101 procedures described elsewhere [26]. The higher heating values (HHV) of the samples
102 were measured using an IKA Calorimeter C200 (IKA, USA), which was performed with
103 approximately 1.0 g of each fuel sample[27] . All experiments were repeated at least
104 twice and the obtained results from these analyses were averaged. The ultimate
105 analysis (CHNS/O) of the parent fuels was conducted using a PE 2400 Series II
106 CHNS/O Analyzer (PerkinElmer, USA) while the oxygen content was obtained by
107 finding the difference[26].

108 2.2.2 Mineral Composition

109 Mineral composition of ash samples of the unblended fuels was determined by using
110 an X-ray Fluorescence (XRF) spectrometer and following the procedure described
111 elsewhere [26]. The mineral composition of the raw oat straw and the water leached
112 sample was also obtained using the XL3t X-ray Fluorescence (XRF) spectrometer
113 (ThermoFisher Scientific, USA).

114 2.3 Combustion Characteristics

115 2.3.1 Thermal Analysis

116 Combustion characteristics of individual fuels and their blends were investigated using
117 a non-isothermal technique which was also adopted by previous research [28, 29].
118 The samples were heated in air (80 vol% Nitrogen and 20 vol% Oxygen) from 50 –
119 900 °C at a heating rate of 20 °C min⁻¹ and a gas flow rate of 50 ml min⁻¹. Peak
120 temperature (PT) was determined as the temperature at which the weight loss ($\frac{dw}{dt}$) of
121 the sample reached its maximum. Burnout temperature (BT) was defined as the
122 temperature at which the rate of burnout (mass loss rate) decreased to less than 1 wt%
123 min⁻¹ on weight basis.

124 2.3.2 Kinetic Study

125 Celaya, Lade [30] argued that the kinetic parameters of the combustion process of
126 coal and biomass blends can be well described by a first order reaction. This is similar
127 to the observations by others [31, 32] who found that the first order reaction model is
128 the most effective solid-state mechanism responsible for co-combustion and co-
129 pyrolysis and activation energies are well represented by a first order Arrhenius plot.
130 Activation energy and pre-exponential factor can be calculated using TGA data
131 collected for non-isothermal kinetics detailed elsewhere [33] [34].

132 The degree of thermal conversion, α , can be defined as

$$133 \quad \alpha = \frac{w_0 - w}{w_0 - w_\infty} \quad (1)$$

134 where w_0 is the initial mass in mg, w is the mass of sample at time, t and w_∞ is the
135 final mass of sample in mg. The reaction rate constant, k is expressed as:

$$136 \quad k = A \exp\left(-\frac{E}{RT}\right) \quad (2)$$

137 where R is the gas constant ($8.314 \text{ J K}^{-1} \text{ mol}^{-1}$), T is the temperature (K), A is the pre-
138 exponential factor (min^{-1}), and E is the activation energy (kJ mol^{-1}).

139 Using the differentiated law of conservation of mass, kinetic equation can be
140 expressed as:

$$141 \quad \frac{d\alpha}{dt} / (1 - \alpha) = A \left(\exp\left(-\frac{E}{RT}\right) \right) \quad (3)$$

142 where α is conversion over a time span.

143 The kinetic parameters were then calculated based on conversions between 1% and
144 30%. This is due to the beliefs about the best region to measure reaction kinetics [35].

145 2.3.3 Catalytic Effect of Biomass Ash

146 To determine the influence of minerals in biomass-derived ash on combustion process,
147 organic compounds of oat straw was burnt out at a temperature below 150°C using a
148 plasma cleaner (PR300, Yamato Scientific, Japan) to prepare low temperature ash of
149 oat straw (OS_LTA). The OS_LTA was then blended with all coal samples at 0.8 and
150 2.8 wt% on a weight basis and the thermal analysis of these blends was then carried
151 out. The blending ratio of the ash was chosen based on the ash content of the 10 and

152 30wt% oat straw blends (0.7 and 2 wt%) and normalizing the blend to 100wt%. Hence,
153 97.2wt% coal + 2.8wt% OS_LTA can be used to mimic the thermal behaviour of 70
154 wt% coal + 2wt% OS_LTA. This will help in determining the degree of catalytic impact
155 of biomass ash on combustion characteristics of the coal sample. The low temperature
156 ashing of oat straw was performed using methods detailed elsewhere [36].

157 2.3.4 Non-Catalytic Effect of Oat Straw

158 The influence of the organic constituents of biomass on the combustion process was
159 determined by blending the coal samples with demineralized oat straw. The
160 demineralisation process via water leaching was performed as in previous study [37].
161 Approximately 5 grams of oat straw was washed using ultra-pure water at 90°C for 2
162 hours. The sample was rinsed and then washed again. After this, it was oven dried at
163 60°C for 24 h. This method was used due to its effectiveness in removing catalytic
164 elements such as potassium and other water soluble salts without affecting other
165 composition of the raw biomass organic components [37]. This demineralised sample
166 (OS_WL) was then blended with the coal samples at 10 and 30 wt% biomass fraction
167 to observe the changes in combustion reaction.

168 2.3.5 Synergy Indicator

169 The degree and extent of synergy was measured using the synergy factor (S.F) and
170 synergy index (S.I) of the fuel blends. These were calculated based on Equations (4)
171 and (5) as detailed in our previous study [36]. The S.I is a synergy index ($^{\circ}\text{C}^{-3} \text{min}^{-1/2}$)
172 and can be calculated using Equation (4):

$$173 \quad S.I = \frac{1}{t_{p-s}^{0.5} T_b^2 T_p} \times 10^6 \quad (4)$$

$$174 \quad S.F = \frac{S.I_{blend}}{S.I_{coal}} \quad (5)$$

175 where, t_{p-s} is the time difference between the start and the peak of the second
 176 reaction zone (min), T_p is the peak temperature ($^{\circ}\text{C}$), and T_b is the burnout
 177 temperature ($^{\circ}\text{C}$). This index establishes synergistic effect at ($\text{SF} > 1.15$) or additive
 178 behaviour ($0.8 \leq \text{SF} \leq 1.15$).

179 2.3.6 Synergy Combination Efficiency

180 In this work, a weighed fraction approach is adopted to signify the degree of synergistic
 181 effects that can be associated with catalytic and non-catalytic synergy.

$$182 \quad (S.F_{OS_LTA} - 1.15) + (S.F_{OS_WL} - 1.15) = S.F_{Ideal} \quad (6)$$

$$183 \quad \frac{S.F_{OS} - 1.15}{S.F_{Ideal}} = \eta_{Synergy} \quad (7)$$

$$184 \quad \frac{\eta_{synergy} \times S.F_{OS_WL}}{S.F_{OS}} = \%_{non-catalytic\ synergy} \quad (8)$$

$$185 \quad \frac{\eta_{synergy} \times S.F_{OS_LTA}}{S.F_{OS}} = \%_{ncatalytic\ synergy} \quad (9)$$

186 Where $S.F_{OS_LTA}$, $S.F_{OS_WL}$ & $S.F_{OS}$ are the synergistic factors of the OS_LTA, OS_WL
 187 and OS blends at the same blending ratio if not additive; $S.F_{Ideal}$ is the expected ideal
 188 synergistic effect if catalytic and non-catalytic synergistic effects were additive;
 189 $\eta_{synergy}$ is the efficiency of the combined synergistic effects to indicate synergistic
 190 promotion ($>100\%$) or inhibition ($< 100\%$); $\%_{catalytic\ synergy}$ and $\%_{non-catalytic\ synergy}$
 191 represents the percentile contributor of catalytic and non-catalytic synergy respectively.

192 3.0 Results and Discussion

193 3.1 Fuel Properties Analyses

194 Table 1 shows the properties of individual samples. The coal samples have the highest
 195 heating value. Therefore the co-firing of coal with oat straw would lead to the reduction

196 in the amount of heat released and lower combustion temperature if the blend is used
 197 in an existing boilers [38]. The results of the ultimate and proximate analyses of the
 198 individual samples are shown in Table 1 with a standard deviation within ± 1.8 wt%.
 199 The volatile matter content of the oat straw (72.1 wt %) was the highest. All coal
 200 samples used in this study have considerable volatiles of 32.2 wt% (YNC), 41.8 wt%
 201 (ATC) 43.2 wt% (GZC) on a dry, ash-free basis which make them easy to burn.

202 *Table 1 – Ultimate and proximate analysis of fuel samples*

	Oat Straw (OS)	Yunnan Coal (YNC)	Guizhou Coal (GZC)	Australian Coal (ATC)		
Ultimate analysis (wt%)						
Carbon	47.5	86.2	81.8	81.3		
Hydrogen	6.8	5.1	7.7	4.9		
Nitrogen	2.3	1	1.8	1.9		
Sulphur	0.3	1.1	3.3	2.2		
Oxygen (by difference)	43.2	6.6	5.4	9.7		
LHV (MJ kg ⁻¹)	17.6	33.5	36.7	35.5		
Proximate analysis (wt%)						
Moisture	4	4.5	1.8	0.7		
Volatile Matter (VM)	72.1	27.2	30.2	34.6		
Fixed Carbon (FC)	17.4	57.3	39.6	48.2		
Ash	6.5	11	28.4	16.5		
Mineral Composition (%wt)						
	OS _{ash}	YNC _{ash}	GZC _{ash}	ATC _{ash}	OS _{raw}	OS_WL
Al ₂ O ₃	0.3	14.5	12.5	39.7	0.3	1.1

SiO ₂	17.8	30.4	30.1	43.2	9.2	43.1
Fe ₂ O ₃	0.3	12.1	18.7	7.5	1.5	-
CaO	3.3	34.1	27.9	4.3	14.8	42.0
K ₂ O	29.2	1.5	6.8	0.8	49.2	8.4
MgO	3.2	0.9	1.7	2.2	0.0	5.4
TiO ₂	-	2.7	1.9	-	-	-
Cl	31.2	-	-	-	25.0	-
Na ₂ O	14.6	3.8	0.4	2.3	-	-

203 All coal samples have relatively high sulphur content (>1wt%) which normally lead to
204 the release of SO_x during combustion. However, the formation of sulphates from the
205 reaction of coal with biomass AAEMs has been discovered to promote the capture of
206 gas phase sulphur which reduces SO_x pollutants [39]. The overall Ca, Na and K
207 content in OS_{raw} is 64 wt% which illustrates high potential in pollution abatement such
208 as sulphur fixing.

209 3.2 Fuel Thermal Behaviour

210 3.2.1 Individual Fuels

211 Oat straw (OS) has two thermal decomposition stages with the first stage starting at
212 144°C and ending at 420°C as shown in Figure 1(a). This stage is linked with the
213 release of volatiles via the decomposition of hemicellulose, cellulose and partial
214 decomposition of lignin [20, 29]. This stage is the main mass loss region due to the
215 high volatile content of oat straw with a peak temperature at 299°C. The second
216 decomposition stage starts at 432°C and ending at 518°C represents mainly the
217 oxidation of the char, which indicates decomposition of remaining lignin.

218 The coal samples, on the other hand, have only one decomposition stage due to the
 219 overlapping release of volatile matters and burning of fixed carbon. This main thermal
 220 degradation took place at 329 – 605°C, 329 – 610°C and 324 - 636°C for YNC, GZC
 221 and ATC respectively with only a single peak appearing at 536°C, 495°C and 533 °C
 222 in that order. The degradation curves of the unblended fuels are shown in Figure 1
 223 with more details on Table 2. As the reactivity of the fuel is inversely proportional to
 224 the peak temperature, the lower PT of OS can be taken as an indicator of its higher
 225 reactivity [40]. Similarly, the low PT of the fuel is linked to the high volatile content of
 226 OS and this can be further associated with its high oxygen/carbon ratio. The lower PT
 227 of GZC can be linked to its high hydrogen content which enhances reactivity
 228 immensely by promoting fuel breakdown into volatiles and gas molecules that burn
 229 more easily.

230 *Table 2 – Combustion characteristics of individual fuels and their blends*

	First Reaction Zone		Second Reaction Zone		Burnout Temperature (°C)
	Temperature range (°C)	Peak Temperature (°C)	Temperature range (°C)	Peak Temperature (°C)	
100wt% OS	144 - 420	299	432 - 518	474	518
100wt% YNC			329 - 605	535	605
90wt%YNC +10wt%OS	244 - 334	304	339 - 591	515	591
70wt%YNC +30wt%OS	201 - 345	301	353 - 583	483	583
100wt% GZC			329 - 610	495	610

90wt% GZC +10wt%OS	246 - 342	315	342-600	480	600
70wt% GZC +30wt%OS	193 -355	302	355 - 589	475	589
100wt% ATC			324 - 636	533	636
90wt% ATC +10wt%OS	257 - 333	309	333 - 625	521	625
70wt% ATC +30wt%OS	204 - 352	301	352 - 606	504	606

231

232 In the char oxidation stage, the burnout temperature and the width of the exothermic
233 curve are two factors for describing fuel reactivity. The width of 86°C for OS, 276°C
234 for YNC , 281°C for GZC and 312°C for ATC conveys the fast progression to burnout
235 of oat straw and the slow burnout of the coal samples with ATC showing the slowest
236 burnout properties.

237 3.2.2 Coal and Biomass Blends

238 The decomposition curve of blends is shown in Figures 1(b)-(d) and the details of the
239 thermal analysis results are provided in Table 2 (standard deviation of the
240 characteristic temperatures of the individual fuels and blends remained within $\pm 1.1\%$).
241 All blends are represented with two peaks, the first is representative of the first
242 reaction zone of unblended OS devolatilization stage (301 - 315°C) while the second
243 peak is linked mainly to coal combustion. The second peak temperature and burnout
244 temperature of the blends revealed an evident reduction in the reaction zone and peak

245 position with increase in the blended OS. This reduction indicates an improvement in
246 fuel reactivity.

247 The improvement noticed in the YNC/OS blends can be categorised in terms of
248 reductions in the 2nd peak temperature which ranged from 20 – 52 °C for the 10 wt%
249 to 30 wt% YNC/OS blends. Relative to this, the extent of burnout temperature
250 reductions is minimal (14 - 22°C). Similarly, the GZC/OS and ATC/OS blends also
251 showed a similar trend of the 2nd PT reductions ranging from 12 - 29°C and BT
252 reductions of 10 - 29°C with increasing OS blend. This reduction in the maximum mass
253 loss temperature of the blends could be linked to the reduced coal char in the blends
254 with increasing biomass content or the increase in reactivity of the coal char due to the
255 release and burning of volatiles introduced by OS during the first reaction stage.
256 Nonetheless, the blending with OS shifted the coal char burnout stage to lower
257 temperatures compared to the unblended coal sample and the extent of this reduction
258 varies for different coal samples and for different blend ratios. In addition to the burnout
259 temperature reduction, the burnout width reduces from 276°C for 100 wt% YNC to
260 230°C (46°C reduction) for 70 wt% YNC + 30 wt% OS blend. Likewise, there were
261 reductions of 48 and 58°C for 30 wt% OS blended with GZC and ATC respectively.
262 These reductions in the width of the exothermic peak of the burnout stage which
263 decrease with an increase in oat straw blending ratio are indicative of less burnout
264 time and higher combustion reactivity.

265 3.2.3 Synergy in Coal/OS blends

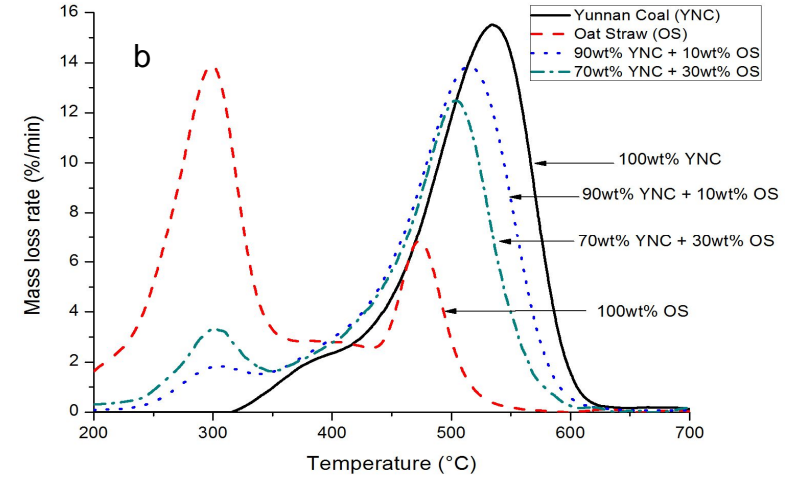
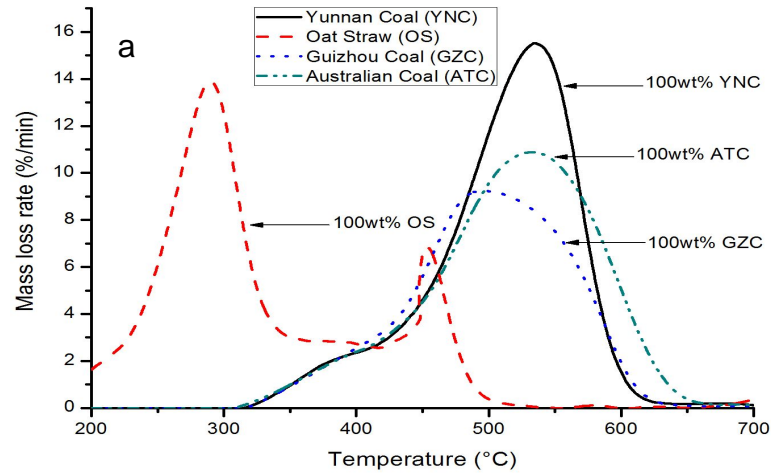
266 Synergy during the thermal reaction of fuel blends has been defined as any positive
267 deviation in the experimental results when compared to the expected results based on
268 individual fuel contributions [41]. Consequently, to verify that the reductions in the 2nd
269 PT and BT of the fuel blends represent interactions between the coal and oat straw

270 samples which lead to synergistic effects, the theoretical data was calculated and
271 compared assuming the interactions between the fuel blends remained additive, which
272 are illustrated in Figure 2(a) – (f).

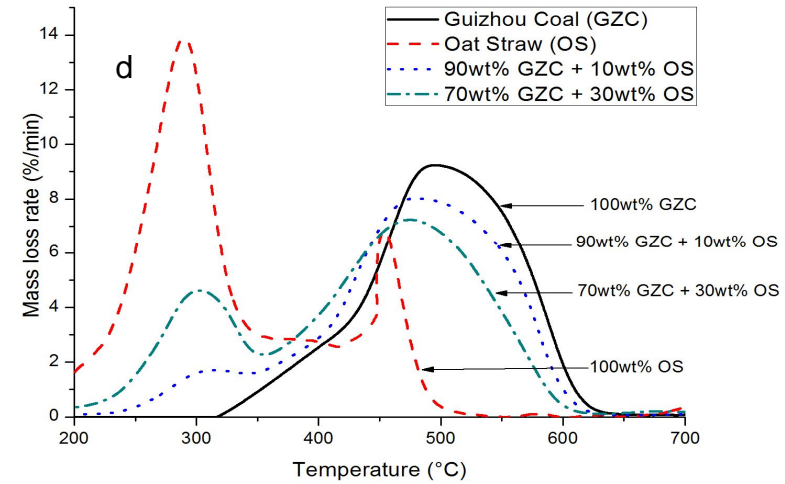
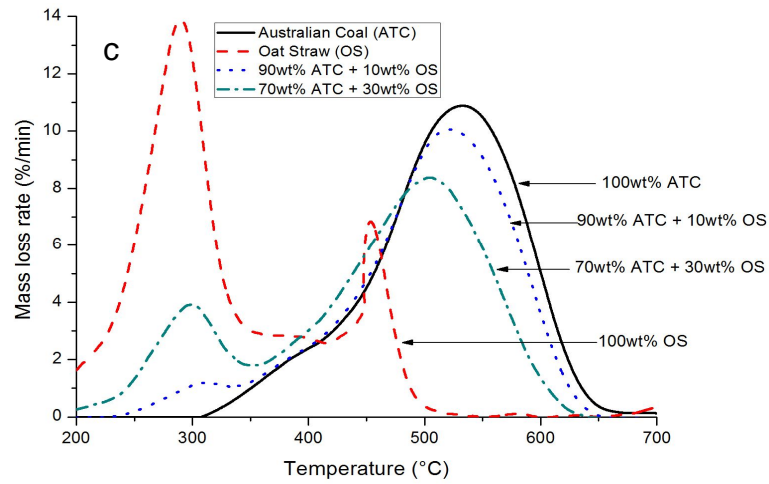
273 The plots in Figure 2(a) – (f) reveal noticeable difference between the theoretical data
274 and the experimental results, thereby corroborate the presence of synergistic
275 interactions in these blends except the 90 wt%ATC +10 wt% OS (Figure 2(e)) which
276 showed almost additive properties. The trend observed includes a greater mass loss
277 area at lower temperatures, lower peak and burnout temperatures in the experimental
278 results compared with the theoretical data. Similar improvements were observed by
279 past studies [19, 42, 43]. Yet, the mechanism of synergy improvement is still unclear
280 due to the conflict in the literature, and the difference in extent and even the causative
281 factors of synergy.

282 The synergy observed by these fuel blends can be linked to either catalytic (due to the
283 volatile inorganic AAEMs present in biomass) and/or non-catalytic (due to the free
284 radicals / hydrogen transfer introduced by the biomass volatiles during thermal
285 reaction) influence [44]. Due to the high AAEMs (62 wt% AAEMs in OS_{raw}) and high
286 volatile matter content of oat straw as shown in Table 1, both mechanisms of synergy
287 could be prominent in these blends. In addition, the structural porosity of the fuel chars
288 obtained after devolatilization may contribute to synergistic effects, by accelerating
289 char combustion, enhancing char burnout and reducing unburnt carbon yield [45, 46].
290 All these factors contribute significantly to the improved combustion efficiency during
291 boiler operation.

292



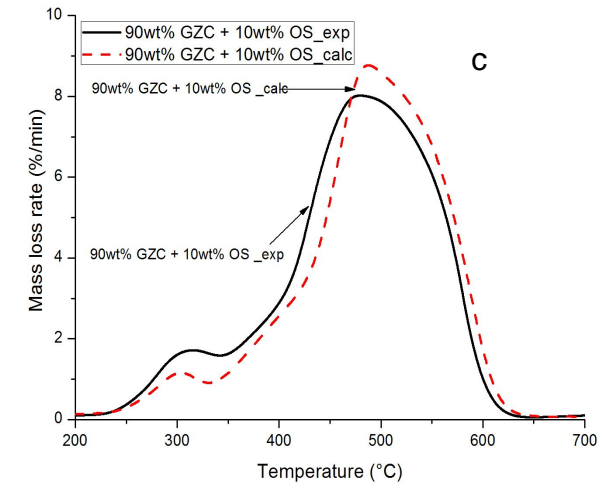
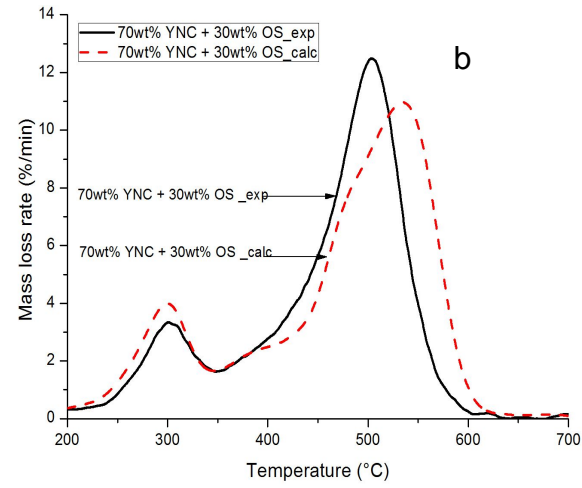
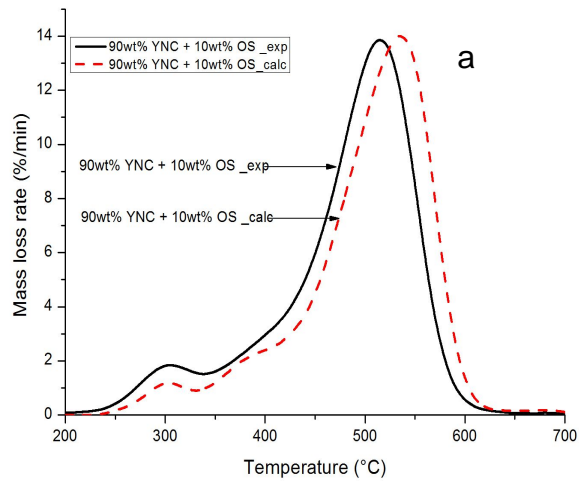
293



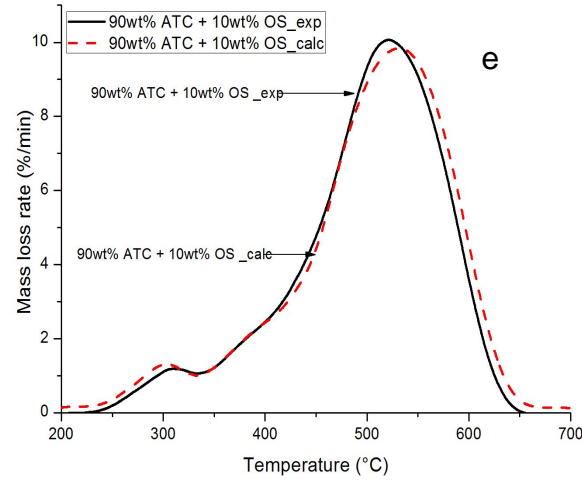
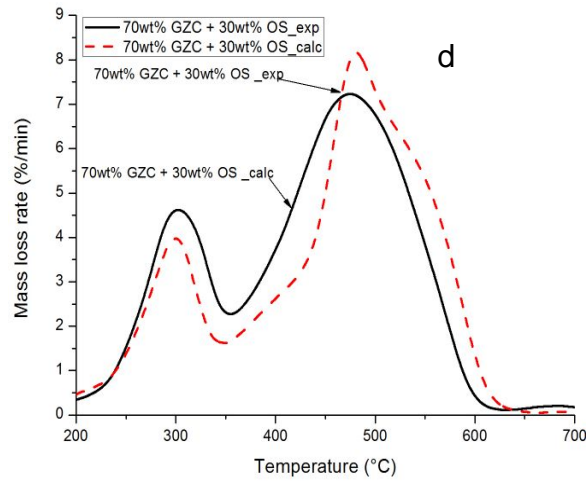
294
295

Figure 1: The DTG curves of (a) individual samples, (b) Yunnan coal /oat straw blends, (c) Australian coal /oat straw blends; and (d) Guizhou coal /oat straw blends.

296



297



298

Figure 2: The DTG curves of the calculated and experimental results of the coal and oat straw blends

299 3.2 Kinetic Study

300 The kinetic model involves the analysis of the two independent reaction zones for the
 301 main fuels and their blends (Table 3). The first zone represents the initial
 302 decomposition of fuel to form volatiles and char. This occurs simultaneously with the
 303 burning of volatiles while the second zone is the burning of char. The activation energy
 304 and pre-exponential factors for the blends and unblended fuels are given in Table 3.
 305 The highest activation energy for both conversion regions analysed was 196.6 kJ/mol
 306 for the second reaction zone of OS. This can be explained by the lower reactivity of
 307 the lignin which makes up the char degradation zone of OS. The lowest activation
 308 energy was obtained for the devolatilisation stage of the OS (52.6 kJ/mol). This low E
 309 can be associated with the initial C-H and C-O bonds associated with volatile matter
 310 combustion and minor C=C bonds. This is because the reaction in the first
 311 decomposition stage of biomass proceeds mostly in the gaseous phase and this is
 312 indicative of lower activation energy.

313 The activation energy for the 1 – 30% conversion of the coal samples remained similar
 314 within the range of 63.7 – 73.1 kJ/mol with 100wt% GZC having the highest value.
 315 This is due to the high carbon content of coal and the condensed carbon structure and
 316 predominant C=C bonds in coal samples [32].

317 Table 3 – Kinetic analysis of fuel and fuel blends.

Sample	Reaction Zone 1			Reaction Zone 2		
	E (kJ mol ⁻¹)	A (min ⁻¹)	R ²	E (kJ mol ⁻¹)	A (min ⁻¹)	R ²
100wt% OS	52.6	1.72E+04	0.97	196.0	3.52E+13	0.92
100wt% YNC				65.0	3.31E+03	0.95

90wt%YNC +10wt%OS	88.8	5.76E+07	0.94	61.5	2.54E+03	0.98
70wt%YNC +30wt%OS	74.8	2.65E+06	0.95	70.8	3.15E+04	0.99
100wt% GZC				73.1	1.96E+04	0.98
90wt% GZC +10wt%OS	103.9	2.14E+09	0.99	69.6	1.42E+04	0.97
70wt% GZC +30wt%OS	80.3	1.18E+07	0.97	64.3	7.69E+03	1.00
100wt% ATC				63.7	2.75E+03	0.98
90wt% ATC +10wt%OS	102.9	1.35E+09	0.99	61.0	2.02E+03	0.99
70wt% ATC +30wt%OS	86.2	3.93E+07	0.98	62.4	3.83E+03	0.99

318

319 The addition of oat straw to coal samples results into two reaction zones with the
320 activation energy of the first reaction zone of all the fuel blends (74.8 – 103.9 kJ/mol)
321 which is remarkably higher than that of the first stage of the 100wt% OS (52.6 kJ/mol).
322 This increase in energy barrier could be associated with the interactions and molecular
323 collisions of oat straw and coal particles during the devolatilisation stage. The fuel
324 blends have 10 – 30% oat straw contents, thereby reducing the quantity of reacting
325 molecules (oat straw's hemicellulose and cellulose) with adequate energy to
326 participate in reaction during this first stage. This will actively reduce the rate of
327 reaction, hence increase the activation energy. This is further verified as the E value
328 obtained reduces by a factor of 8.2 – 23% with an increase in the oat straw blended
329 from 10 to 30 wt%.

330 Furthermore, the activation energy of the second reaction zone remained lower than
331 those of the 2nd reaction zone of OS (196.6 kJ/mol) and the main reaction zone of the
332 coal samples except for the 70wt% YNC blend. Similar to the first reaction zone, the
333 activation energy reduces with an increase in oat straw blend ratio for most of the
334 blends with the exception of 70wt% ATC and 70wt%YNC blend. The slight increase in
335 both blends can be explained by the increase in the lignin component from the higher
336 OS blending ratio. The reduction in activation energy could be linked to the tendency
337 of the C-H and C-O bonds of biomass (during devolatilisation) interacting with and
338 promoting the breakage of the C=C bonds of coal char, thereby accelerating the char
339 oxidation and reducing the activation energy [32]. The reduction in activation energy
340 of the 2nd reaction stage is clearly not additive as it remains lower than that of both 100
341 wt% OS and 100 wt%YNC. This could also be indicative of catalytic synergistic effect
342 of mineral matter in biomass which promotes char burnout .

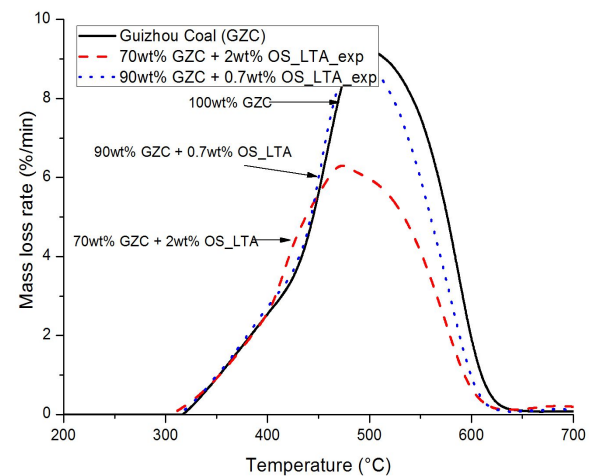
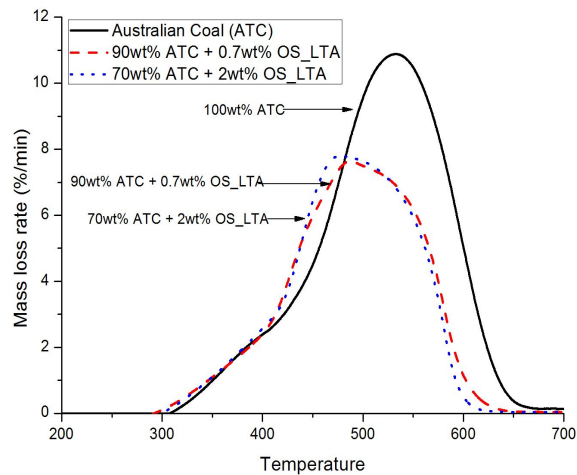
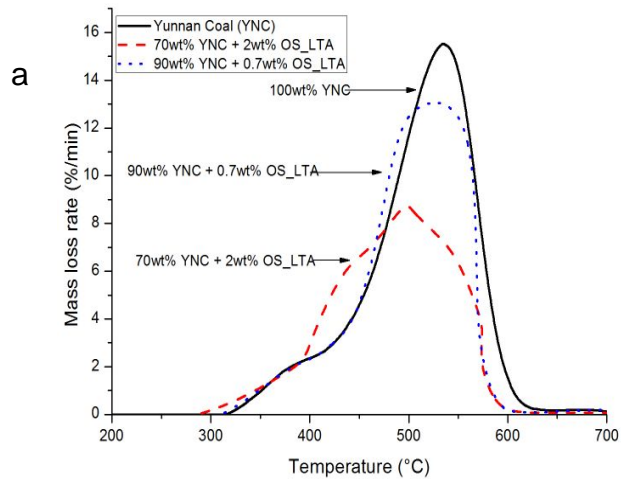
343 The pre-exponential factor is dependent on the rate of collision between the fuel
344 molecules during the thermal reaction [47]. The frequency factor obtained in the first
345 reaction zone of the fuel blends remained higher than that of 100 wt% OS and it
346 reduces with the increase in OS blending ratio. This high pre-exponential factor could
347 indicate that a high fraction of the collisions between the oat straw volatiles and coal
348 do not result in any reactions due to the lack of adequate energy to react. In the second
349 reaction zone, most of the frequency factor remained lower than that of the parent
350 fuels. Since this factor is mainly dependent on reaction concentration, the reduction in
351 frequency factor with the increase in biomass blending ratio is logical due to the lower
352 concentration of reactants (mainly YNC char) at the second reaction zone. Likewise,
353 the collision frequency reduces from the first reaction zone to the second reaction zone
354 of the fuel as there would be decrease in reactant with the progression of the reaction.

355 3.3 Catalytic Synergistic Effect

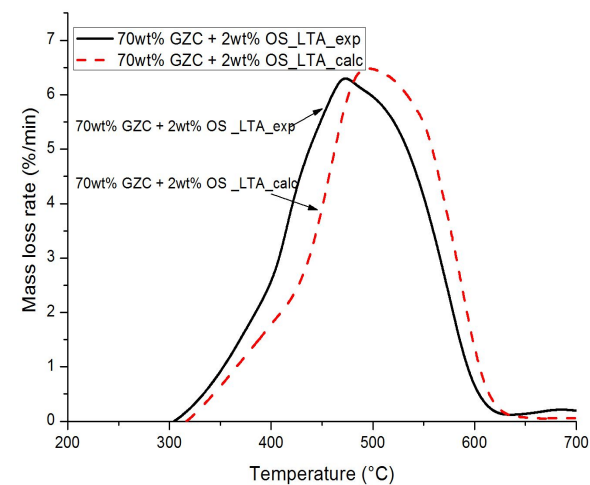
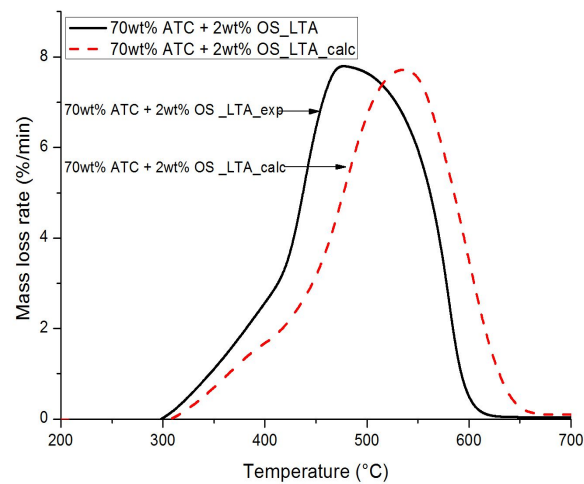
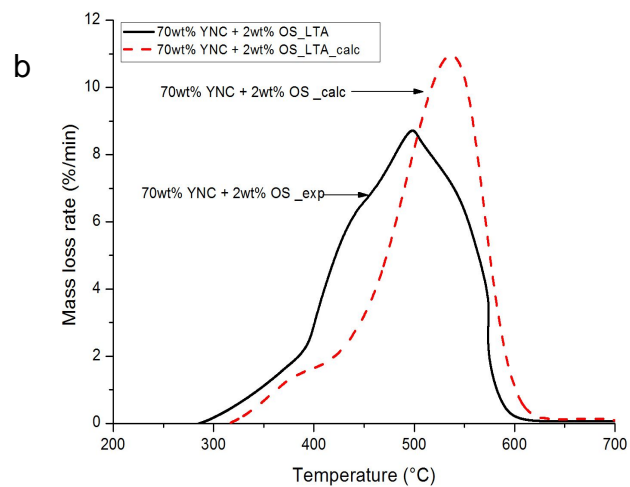
356 The synergistic effects denoted by the reductions in peak and burnout temperatures
357 of the fuel blends can be linked to either catalytic or non-catalytic effects. To
358 understand the catalytic effects, the coal samples were blended with low temperature
359 ash of oat straw (OS_LTA) at different blending ratios. This approach aids in isolating
360 the catalytic effect of the minerals from oat straw on organic constituents'
361 decomposition of the coal samples. Therefore, OS_LTA was blended at 0.7 and 2%
362 wt fraction with YNC, GZC and ATC and their combustion results are provided in Table
363 4. The peak and burnout temperatures reduced by 8 – 56°C and 10 - 43°C respectively
364 with increasing OS_LTA content. The highest reduction from catalytic OS_LTA was
365 detected in ATC. This confirms the presence of catalytic improvement when the
366 organic elements from coal interact with the AAEMs from OS. These reductions in
367 peak temperatures are expected to influence ignition temperature as well. The major
368 influencer of this catalytic synergistic effect is potassium due to its high content (49.2
369 wt%) in oat straw (Table 1). Furthermore, the volatility of potassium will be enhanced
370 by the presence of chlorine (25wt % in OS_{raw}), thereby reacting to readily form KCl
371 during combustion. Apart from chlorides, other route of volatilising potassium and
372 other reactive inorganic AAEMs with catalytic effects includes gaseous phase release
373 in form of ions or hydroxides. This has been extensively studied by Van Lith, Jensen
374 [48] and Mason, Darvell [49] . More details on catalytic synergy has been described
375 in previous studies [50].

376 The weight fraction of OS_LTA used in the blends were selected based on the OS ash
377 contents in the coal/OS fuel blends. Therefore, the results obtained can be mildly
378 compared with that individual coal samples to demonstrate the catalytic synergistic
379 effect of oat straw on the blends. This comparison is shown in Figure 3 along with the

380 validation of synergy by comparing the experimental results with calculated theoretical
381 data for the 70wt% coal + 2wt% OS_LTA blends. As shown in Fig 3(b), there is a
382 significant shift of mass loss towards lower temperature. This confirms the catalytic
383 synergistic effects which promote the decomposition of coal char into low molecular
384 weight species that can easily burn. The catalytic synergistic effect thereby enhance
385 char reactivity with better burnout properties [44].



386



387

388
389

Figure 3: The DTG curves of (a) coal samples and oat straw low temperature ash blends; and (b) calculated and experimental results of the 70wt% coal and 2wt% oat straw low temperature ash blends

390 The PT of the YNC/OS_LTA and GZC/OS_LTA blends appear within $\pm 15^\circ\text{C}$ in
 391 comparison to the YNC/OS and GZC/OS blends. In contrast, the PT of ATC/OS_LTA
 392 blends remained lower by 27 - 34 $^\circ\text{C}$ and BT by 10 - 22 $^\circ\text{C}$ compared with ATC/OS
 393 blends. This shows that different degree of improvement is observed by different coal
 394 types with ATC having the most significant improvement due to catalytic synergistic
 395 effect.

396 *Table 4 – Combustion characteristics of coal samples and low temperature ash blends*

	Temperature range ($^\circ\text{C}$)	Peak Temperature ($^\circ\text{C}$)	Burnout Temperature ($^\circ\text{C}$)
100wt% YNC	329 - 605	535	605
90wt% YNC + 0.7wt% OS_LTA	324 - 584	527	584
70wt% YNC + 2wt% OS_LTA	308 - 582	498	582
100wt% GZC	329 - 610	495	610
90wt% GZC + 0.7wt% OS_LTA	327 - 600	486	600
70wt% GZC + 2wt% OS_LTA	324 - 593	473	593
100wt% ATC	324 - 636	533	636
90wt% ATC + 0.7wt% OS_LTA	313 - 603	487	603
70wt% ATC + 2wt% OS_LTA	316 - 593	477	593

397 This provides credence to the presence and contributions of the catalytic synergistic
 398 effect during the co-firing of biomass and coal. It also proves that the cofiring coal with

399 biomass of high AAEMs content could improve the overall combustion performance of
 400 the blends by taking advantage of the catalytic synergistic effects.

401 3.4 Non-catalytic Synergy Effects

402 Now that the extent of catalytic synergy has been isolated in the fuel blends, a similar
 403 method can be used for separating the non-catalytic synergy effect using water
 404 leached oat straw (OS_WL) blended with the coal samples. The results are outlined
 405 in Figure 4 and Table 5. The water leaching of oat straw (OS_WL) led to the complete
 406 removal of Fe and Cl, 95 - 96% reduction in K and 19 – 39% reduction in Ca as seen
 407 in Table 1 while the SiO₂ and Al₂O₃ content of OS_{raw} remained unchanged due to their
 408 high thermal stability and insolubility in water. In this washing process, the reduction
 409 in Ca is less due to the presence of thermally stable and water insoluble compounds
 410 such as CaCO₃. However, this does not affect the studied reaction zones. The non-
 411 catalytic mechanism of synergistic improvement is primarily established from volatiles
 412 which promotes the reaction via hydrogen donation to coal's free radicals, thereby
 413 improving reactivity of char formed.

414 *Table 5 – Combustion characteristics of coal samples and water leached oat straw blends*

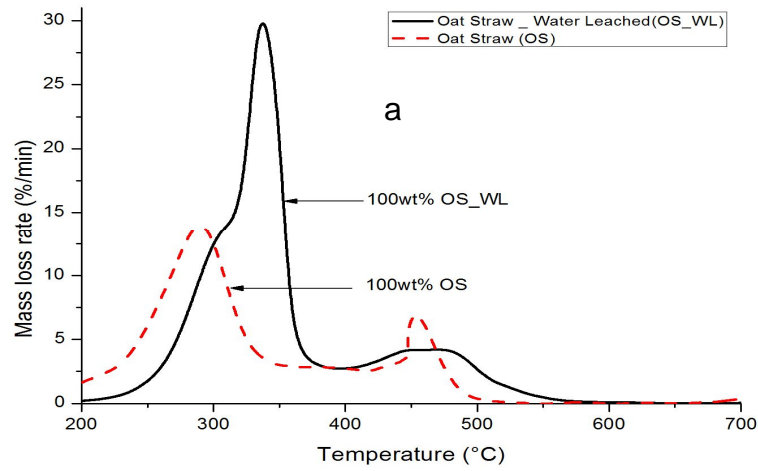
	First Reaction Zone		Second Reaction Zone		Burnout Temperature (°C)
	Temperature range (°C)	Peak Temperature (°C)	Temperature range (°C)	Peak Temperature (°C)	
100wt% OS	211-396	337	396 - 532	471	532
100wt% YNC			329 - 605	535	605
90wt% YNC + 10wt% OS_WL	274 - 374	343	374 - 589	509	589

70wt%YNC + 30wt% OS_WL	252 - 379	332	379 - 582	511	582
100wt% GZC			329 - 610	495	610
90wt% GZC + 10wt% OS_WL	280 - 361	337	361 - 598	494	598
70wt% GZC + 30wt% OS_WL	251 - 376	339	376 - 597	502	597
100wt% ATC			324 - 636	533	636
90wt% ATC + 10wt% OS_WL	274 - 359	334	359 - 611	511	611
70wt% ATC + 30wt% OS_WL	249 - 375	334	375 - 603	513	603

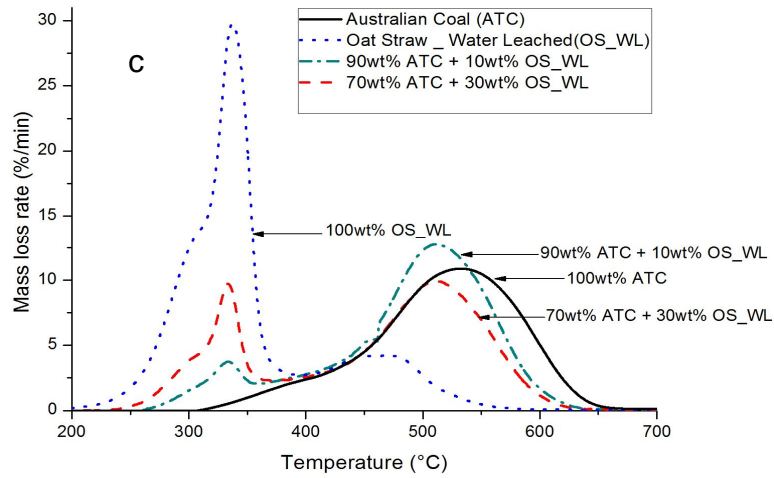
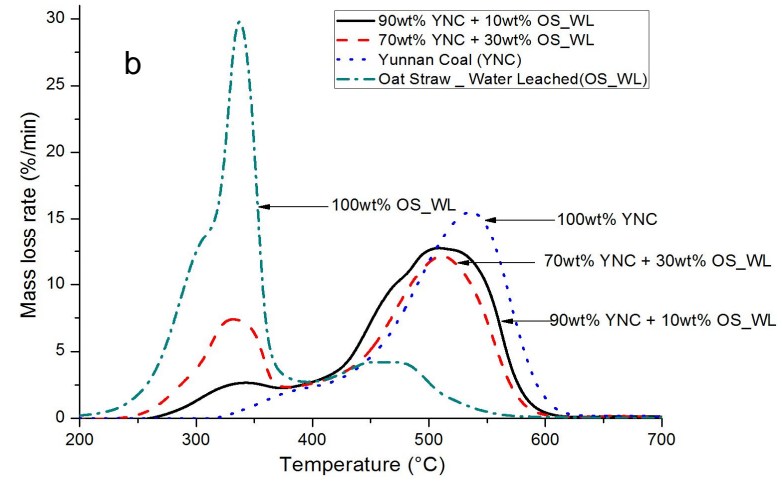
415 A remarkable observation in Figure 4a is the increase in mass loss rate of 100 wt%
416 OS_WL in the first reaction zone and the pronounced shoulder at 313 °C (indication
417 of hemicellulose decomposition) in comparison to 100 wt% OS. This transformation is
418 evident, implying that the effect of AAEMs present is a shift in devolatilization to lower
419 temperature range at lower volatility. All these are similar to the observations of Le
420 Brech, Ghislain [37] for the effect of demineralisation (specifically, potassium removal)
421 on the thermal decomposition of biomass. The improvement in burnout properties due
422 to catalytic AAEMs is clear with the slow burnout in the 2nd reaction zone of OS_WL.
423 Similar to the ash blends, different ranges of reduction was observed in the blends.
424 The unblended OS_WL has its peak and burnout temperatures at 337/471°C and
425 532°C respectively with the 1st PT about 38°C greater than that of OS. Similarly, the
426 BT of OS_WL increased by 14°C compared to the OS. This suggests the impact of

427 mineral matter in the low peak and burnout temperature observed initially in
428 100wt%OS.

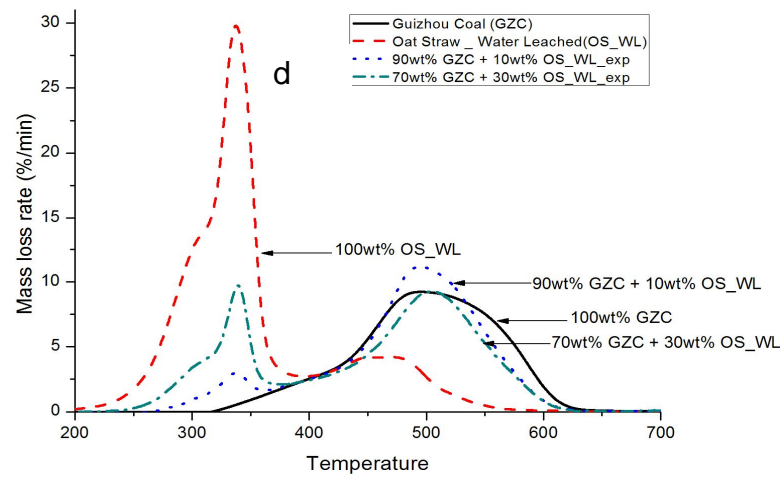
429 The first PT of the coal/OS_WL blends remained within $\pm 6^\circ\text{C}$ of that of the OS_WL
430 fuel, hence maintaining additive behaviour in the first reaction zones. The
431 ATC/OS_WL and YNC/OS_WL exhibited significant improvement with reductions in
432 the 2nd PT and BT of the blends in the range of 20 – 26°C and 16 – 33°C respectively.
433 It is noteworthy that this PT remained similar ($\pm 2^\circ\text{C}$) with an increase in the OS_WL
434 blend ratio. This indicates that the influence of OS organic constituents on the
435 improvement in maximum char degradation temperature is invariable and does not
436 decrease progressively with blending ratios as seen in the OS and OS_LTA blends.
437 In addition, the BT decreases with an increase in blending ratio. This suggests the
438 impact of organic constituents on the improvement in char burnout. In contrast to the
439 previous two blends, the GZC/OS_WL blend showed an insignificant improvement
440 with the 2nd PT which remained similar to that of the 100 wt% GZC, although there
441 was still a noticeable decrease in BT of 11 - 13°C. This confirms that the extent of
442 synergy is highly dependent on the coal samples.



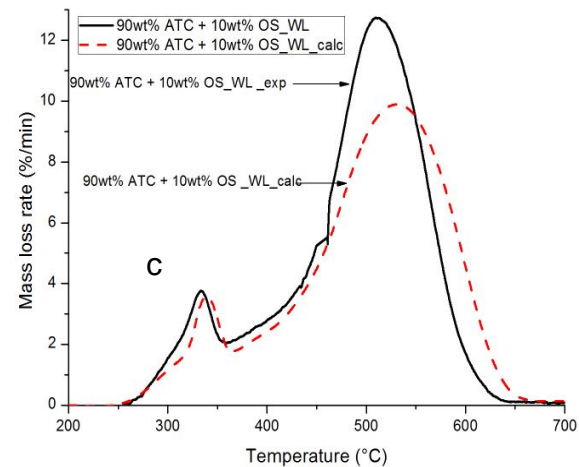
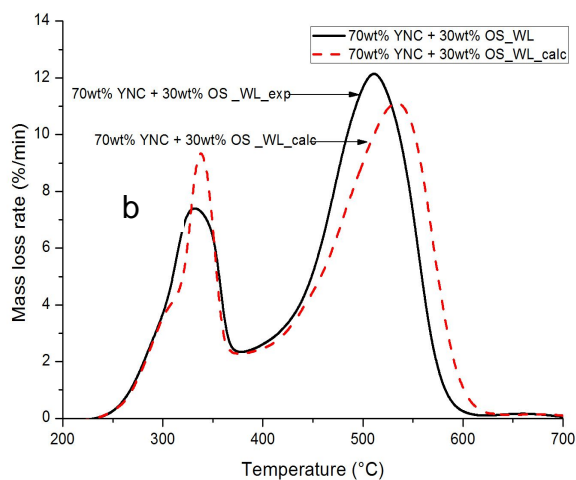
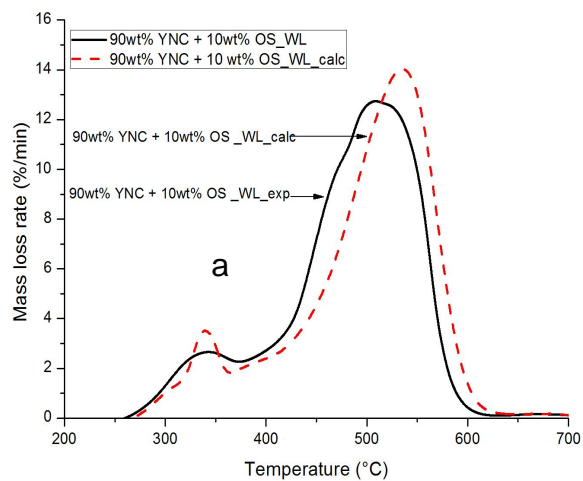
443



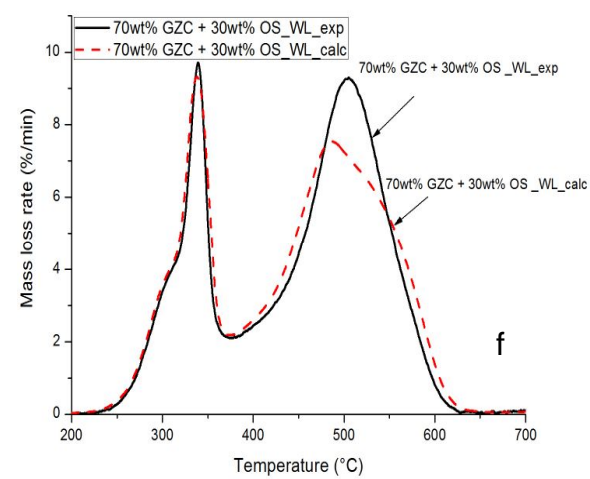
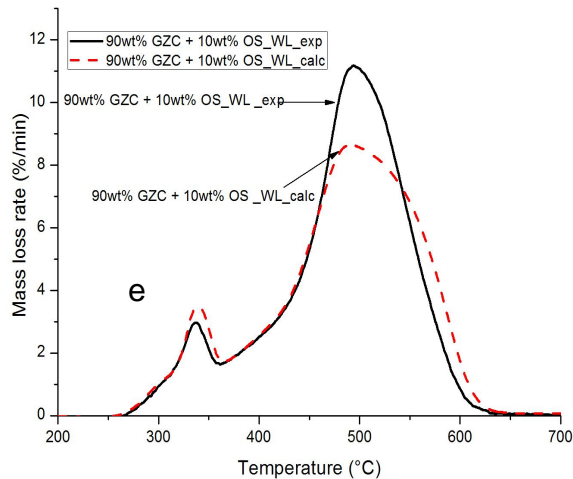
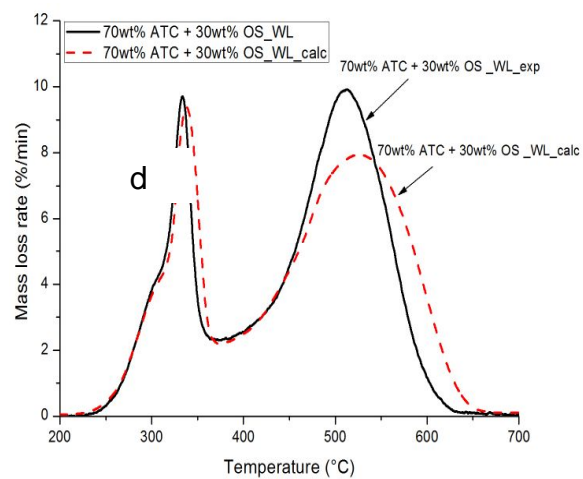
444



445 Figure 4: The DTG curves of (a) OS and OS_WL, (b) Yunnan coal and OS_WL blends; and (d) Guizhou
 446 coal and OS_WL blends.



447



448

449

Figure 5: The DTG curves of the calculated and experimental results of the coal and water leached oat straw blends

450 The main actuator of non-catalytic synergy from biomass is the hydrogen transfer
451 phenomenon which occurs from the cellulose and hemicellulose content of biomass
452 to the coal samples during the release of volatiles [44]. The free radical/hydrogen
453 donation from the volatiles released from biomass reacts with coal's free radical to
454 enhance its thermal decomposition. This results in the formation of products of rather
455 low molecular weight (net increase in volatiles) and generates reduced quantity of less
456 reactive char [51]. This non-catalytic synergy is evident from the Figure 5(a) – (f) where
457 the experimental results have higher mass loss rate at lower temperatures for the 2nd
458 reaction zone of the YNC and ATC blended with OS_WL compared with the theoretical
459 expectation. This increases char reactivity and decreases the PT and BT. However,
460 the GZC blends does not display this property but there is a significant increase in the
461 overall fuel conversion by the increase in mass loss rate. This is because GZC has
462 considerably high hydrogen content (about 50% more than ATC and YNC), thereby
463 limiting the influence of hydrogen/free radicals reaction for this synergistic effects to
464 occur. Irrespective of this, the increase in volatile matter (VM) content present in this
465 fuel blend favours the formation of porous char which promotes solid to gaseous
466 conversion and burnout.

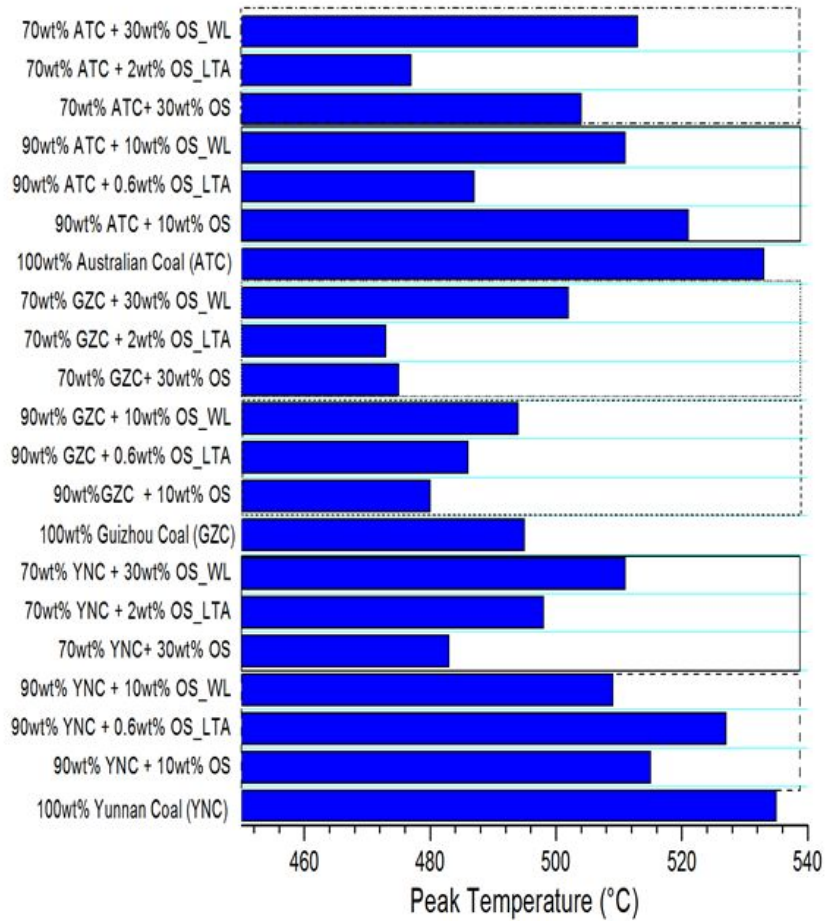
467 3.5 Synergy Index and Synergy combination Efficiency

468 The variations in 2nd peak and burnout temperatures (Figure 6) are not an effective
469 marker for quantifying the extent of synergy. Therefore synergy factor (S.F) was
470 calculated for all the samples as described by Oladejo, Adegbite [36]. This provides a
471 measure of the extent of catalytic, non-catalytic and combined synergistic effect of oat
472 straw on the coal sample. The S.F. results showed that all blends exhibited synergistic
473 effects with $1.99 \geq S.F \geq 1.18$ with the exception of the GZC + 1 wt%OS_LTA which
474 exhibited additive interaction with an S.F of 1.09. Although the increment rate varies,

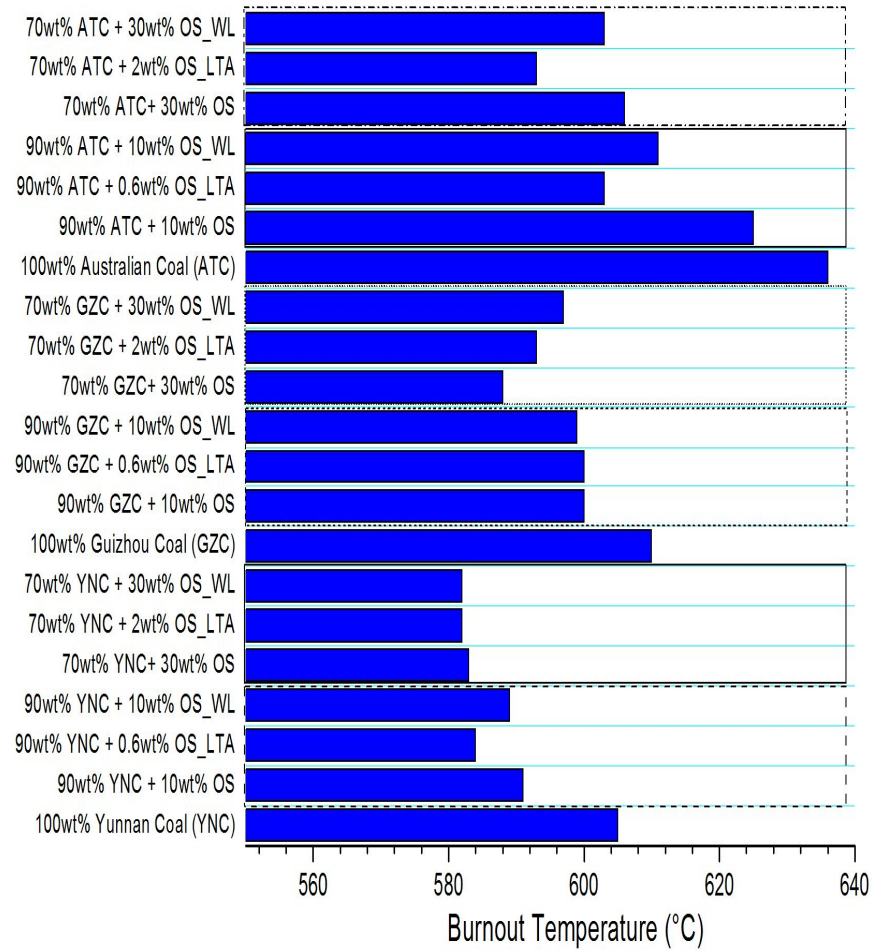
475 the synergy factor of all the blends increased with OS, OS_LTA, and OS_WL blending
476 ratio as shown in Table 6. It is observed that for the 10 wt% OS blends, GZC showed
477 the highest improvement with S.F of 1.34 while for the 30 wt% OS blends; ATC
478 exhibited a S.F of 1.61 representing the highest synergistic effect. This result confirms
479 that the blend with the highest S.F indicates greater improvement in combustion due
480 to both the non-catalytic and catalytic synergistic effects.

481 As previously showed, the ATC/OS_LTA blends showed the highest degree of
482 catalytic synergy (S.F of 1.72 – 1.90) for both blending ratios while the GZC/OS_LTA
483 blends revealed the lowest extent of synergistic effects (S.F of 1.09 – 1.20). Based on
484 this, it can be inferred that catalytic synergistic effect is higher in ATC and this can be
485 associated with the rank of the coal. This demonstrates previous discoveries by
486 McKee, Spiro [52] that catalytic activity of biomass AAEMs is more evident and
487 increases with coal ranks. In addition to this, the high ash content of GZC increases
488 the potential for the deactivation of catalytic minerals of biomass by the aluminosilicate
489 in GZC. This would result in lower catalytic improvement. Similarly, the observation
490 of non-catalytic synergistic effects reveals that the ATC/OS_WL blends portrays the
491 highest synergistic interaction (S.F of 1.75 – 1.90) and GZC/OS_WL blends with S.F
492 of 1.27-1.28 depicting the smallest degree of improvement. As previously explained in
493 section 3.5, the free radical/hydrogen interaction is very complex, therefore the trend
494 in S.F can be related with the oxygen and hydrogen content of the coal and its ability
495 to form/receive reactive OH and H radicals with mobile H from biomass.

496



497



498

Figure 6: Disparities in the peak and burnout temperature of char burnout zone of the blends

499 From the Table 1, ATC has the lowest hydrogen and highest oxygen content (Oxygen-
500 to-Hydrogen ratio of 2), this increases its potential as a hydrogen recipient.
501 Consequently, GZC has a low Oxygen-to-Hydrogen ratio of 0.7 and that of YNC was
502 1.3 which correlates well with the trend observed.

503 An interesting observation is that the influence of catalytic synergistic effects is lesser
504 in all the blends compared to the non-catalytic synergy apart from the ATC blends in
505 which the catalytic and non-catalytic synergies are evidently comparable. This clearly
506 indicates that non-catalytic synergistic effect is more prominent in these blends rather
507 than catalytic influence of the AAEMs. Another remarkable discovery is that the
508 individual S.F.s of the ATC/OS_LTA and ATC/OS_WL blends remained considerably
509 higher than that of the ATC/OS blend. Similar observation is found in the YNC/ OS_WL
510 blends. This suggests that a level of inhibition is experienced in coal/biomass fuel
511 blends. This could be associated with competitive parallel/sequential reactions that
512 can be termed as “synergy competition”. As explained in sections 3.4 and 3.5, both
513 non-catalytic and catalytic synergistic effects increases the yield of low-molecular
514 weight species by fragmentation, ring opening, and dehydration. In addition, they
515 promote complete decomposition of lighter volatile species which results in the
516 formation of porous and highly reactive char with better burnout properties [36, 37].
517 This would unavoidably lead to an extent of synergy suppression (either catalytic or
518 non-catalytic or both) due to the overlapping of both the organic and inorganic
519 constituent of biomass competing for coal char, making the reaction significantly more
520 perplexing. The limitation in coal reactant to be enhanced, and this competitive
521 reaction will reduce the efficiency and extent of expected synergistic effects. This is
522 quite similar to the observations by other researchers [53] in the catalytic upgrading of
523 bio-oil where the presence of bio-based AAEMs results in competitive reaction which

524 changes product distribution, complicates the reactions and reduces carbon
525 conversion efficiency. More evidence of this occurrence can be related to the work by
526 Le Brech, Ghislain [37] who verified that high potassium content in raw biomass (main
527 contributor to catalytic synergistic effects) led to significant decrease in mobile proton
528 formation, hence H fluidity (non-catalytic influencer). This is through K reacting with
529 the polysaccharide structure and stabilizing the free radicals during the bond cleavage
530 occurring at the devolatilization stage, promoting cross-linking reactions and
531 consequently leads to increase in high-molecular-weight char, thereby reducing
532 overall synergistic effects. As a result, the synergistic effects in the OS/coal blends
533 remained lower than the combination of catalytic and non-catalytic synergistic effects
534 of the OS_LTA and OS_WL fuel blends.

535 The results of the synergy combination efficiency obtained from equations (8) and (9)
536 (section 2.3.6) are shown in Table 6. Interestingly, the result revealed that the highest
537 combined synergistic promotion was observed with an $\eta_{synergy}$ of 194% which was
538 obtained for the 70wt%GZC + 30wt%OS blend. Here, catalytic synergistic effect
539 contributes 30.9% while non-catalytic synergy makes up 69.1%. This simply interprets
540 that the combined improvement obtained in the OS_LTA and OS_WL blends were
541 lower than that observed in the main oat straw blends. The high combined synergy
542 efficiency found could be associated with the low synergy detected in the OS_LTA
543 blend, hence leading to less competitive reaction, which thereby allows effective
544 interaction from the non-catalytic synergistic effects. The GZC/OS blends showed a
545 synergistic combination of both modes of synergy, as the S.F of the GZC/OS remained
546 higher than that of the GZC/OS_LTA and GZC/OS_WL blends. This limited synergy
547 suppression could be associated to the lower maturity of the coal as characterised by
548 its high hydrogen content.

549 The lowest synergy efficiency was realised in the 90wt%ATC +10wt%OS blend with
 550 an efficiency of 2.2% with the contribution of catalytic and non-catalytic synergy of 48.8
 551 and 51.2% respectively. This indicates a higher degree of synergy suppression when
 552 both modes of synergistic effects are highly effective independently. This discovery
 553 could imply that the use of either catalytic biomass ash or highly volatile organic
 554 constituent of biomass separately have the potential to create higher magnitude of
 555 synergistic effects in ATC than raw OS. Similar discovery was shown in YNC blends
 556 to a lesser extent. This is therefore a reduction in synergy combination efficiency with
 557 an increase in coal quality / maturity.

558 *Table 6 – Synergy factor, combined synergy efficiency and catalytic and non-catalytic synergy*
 559 *contributions of the fuel blends*

Sample	Synergy Factor	Combined Synergy Efficiency (%)	Non-Catalytic Synergy (%)	Catalytic Synergy (%)
	<i>S.F</i>	$\eta_{Synergy}$	$\%_{non-catalytic\ synergy}$	$\%_{catalytic\ synergy}$
90wt% YNC + 10wt% OS	1.18	6.7	90.0	10.0
70wt% YNC + 30wt% OS	1.50	60.0	63.7	36.3
90wt% ATC + 10wt% OS	1.18	2.2	51.2	48.8
70wt% ATC + 30wt% OS	1.61	28.7	47.2	52.8
90wt% GZC + 10wt% OS	1.34	141.7	100.0	-
70wt% GZC + 30wt% OS	1.50	194	69.1	30.9
90wt% YNC + 10wt% OS_WL	1.49	--	--	--
70wt% YNC + 30wt% OS_WL	1.52	--	--	--
90wt% ATC + 10wt% OS_WL	1.75	--	--	--

70wt% ATC + 30wt% OS_WL	1.91	--	--	--
90wt% GZC + 10wt% OS_WL	1.29	--	--	--
70wt% GZC + 30wt% OS_WL	1.27	--	--	--
90wt% YNC + 0.7wt% OS_LTA	1.19	--	--	--
70wt% YNC + 2wt% OS_LTA	1.36	--	--	--
90wt% ATC + 0.70wt% OS_LTA	1.72	--	--	--
70wt% ATC + 2wt% OS_LTA	1.99	--	--	--
90wt% GZC + 0.70wt% OS_LT	1.09	--	--	--
70wt% GZC + 2wt% OS_LTA	1.21	--	--	--

560

561 4.0 Conclusions

562 The cofiring of solid fuels for improving energy efficiency and environmental
563 sustainability necessitates explicit understanding of all occurrences during such
564 reaction. This requires further research of potential interactions between the fuels
565 constituents. This study investigates synergistic effects experienced in the blending of
566 oat straw with Yunnan, Guizhou and Australian coals with up to 10% reduction in peak
567 temperatures and up to 17% reduction in activation energy. This would result in
568 thermal/exergy efficiency increase if these blends are utilised in practice with
569 appropriate boiler designs.

570 The catalytic and non-catalytic synergistic effects were analysed independently to
571 measure their individual contributions. The results revealed a degree of synergy
572 inhibition in higher rank coals and synergy promotion were detected in lower rank coals
573 with synergy efficiency ranging from 2.2 – 194%. The synergy inhibition detected was
574 from overlapping function of both catalytic AAEMs and organic contents of biomass in
575 promoting radical propagation for enhancing reactivity in the fuel blends. from
576 overlapping The approach utilized in this study can be useful in optimising synergistic
577 effects and choosing ideal biomass when co-firing with different coal types for
578 enhancing the combustion performance of the blends.

579 **Acknowledgements**

580 The author acknowledges the financial support from the International Doctoral
581 Innovation Centre, Ningbo Education Bureau, Ningbo Science and Technology
582 Bureau, and the University of Nottingham. This work was also supported by the UK
583 Engineering and Physical Sciences Research Council [grant numbers EP/G037345/1
584 and EP/L016362/1]. China's Ministry of Science and Technology is acknowledged for
585 partially sponsoring this research under its major R&D scheme
586 (2017YFB0603202).The Ningbo Bureau of Science and Technology, under its
587 Innovation Team Scheme (2012B82011) and Major R&D Programme (2012B10042)
588 is also acknowledged for its funding.

589 **References**

- 590 [1] International Energy Agency. World Energy Outlook. International Energy Agency; 2007.
591 [2] Dong NS. Utilisation of low rank coals. IEA Clean Coal Centre; 2011.
592 [3] Downward GS, Hu W, Large D, Veld H, Xu J, Reiss B, et al. Heterogeneity in coal composition and
593 implications for lung cancer risk in Xuanwei and Fuyuan counties, China. Environment international.
594 2014;68:94-104.
595 [4] Savolainen K. Co-firing of biomass in coal-fired utility boilers. Applied Energy. 2003;74(3–4):369-
596 81.

- 597 [5] Chen X. Economic potential of biomass supply from crop residues in China. *Applied Energy*.
598 2016;166:141-9.
- 599 [6] Gani A, Morishita K, Nishikawa K, Naruse I. Characteristics of Co-combustion of Low-Rank Coal with
600 Biomass. *Energy & Fuels*. 2005;19(4):1652-9.
- 601 [7] Basu P. Chapter 10 - Biomass Cofiring and Torrefaction. *Biomass Gasification, Pyrolysis and*
602 *Torrefaction (Second Edition)*. Boston: Academic Press; 2013. p. 353-73.
- 603 [8] Nian V. The carbon neutrality of electricity generation from woody biomass and coal, a critical
604 comparative evaluation. *Applied Energy*. 2016;179:1069-80.
- 605 [9] Zhang Q, Li Q, Zhang L, Wang Z, Jing X, Yu Z, et al. Preliminary study on co-gasification behavior of
606 deoiled asphalt with coal and biomass. *Applied Energy*. 2014;132:426-34.
- 607 [10] Priyanto DE, Ueno S, Sato N, Kasai H, Tanoue T, Fukushima H. Ash transformation by co-firing of
608 coal with high ratios of woody biomass and effect on slagging propensity. *Fuel*. 2016;174:172-9.
- 609 [11] Adeyemi I, Janajreh I, Arink T, Ghenai C. Gasification behavior of coal and woody biomass:
610 Validation and parametrical study. *Applied Energy*. 2016.
- 611 [12] Akram M, Tan CK, Garwood DR, Fisher M, Gent DR, Kaye WG. Co-firing of pressed sugar beet pulp
612 with coal in a laboratory-scale fluidised bed combustor. *Applied Energy*. 2015;139:1-8.
- 613 [13] De Laporte AV, Weersink AJ, McKenney DW. Effects of supply chain structure and biomass prices
614 on bioenergy feedstock supply. *Applied Energy*. 2016;183:1053-64.
- 615 [14] Hodžić N, Kazagić A, Smajević I. Influence of multiple air staging and reburning on NO_x emissions
616 during co-firing of low rank brown coal with woody biomass and natural gas. *Applied Energy*.
617 2016;168:38-47.
- 618 [15] Karampinis E, Nikolopoulos N, Nikolopoulos A, Grammelis P, Kakaras E. Numerical investigation
619 Greek lignite/cardoon co-firing in a tangentially fired furnace. *Applied Energy*. 2012;97:514-24.
- 620 [16] Li J, Brzdekiewicz A, Yang W, Blasiak W. Co-firing based on biomass torrefaction in a pulverized
621 coal boiler with aim of 100% fuel switching. *Applied Energy*. 2012;99:344-54.
- 622 [17] Shao Y, Wang J, Xu C, Zhu J, Preto F, Tourigny G, et al. An experimental and modeling study of ash
623 deposition behaviour for co-firing peat with lignite. *Applied Energy*. 2011;88(8):2635-40.
- 624 [18] Xiao H-m, Ma X-q, Lai Z-y. Isoconversional kinetic analysis of co-combustion of sewage sludge with
625 straw and coal. *Applied Energy*. 2009;86(9):1741-5.
- 626 [19] Wu T, Gong M, Lester E, Hall P. Characteristics and synergistic effects of co-firing of coal and
627 carbonaceous wastes. *Fuel*. 2013;104:194-200.
- 628 [20] Vamvuka D, Sfakiotakis S. Combustion behaviour of biomass fuels and their blends with lignite.
629 *Thermochimica Acta*. 2011;526(1-2):192-9.
- 630 [21] Lester E, Gong M, Thompson A. A method for source apportionment in biomass/coal blends using
631 thermogravimetric analysis. *Journal of Analytical and Applied Pyrolysis*. 2007;80:111-7.
- 632 [22] Sjostrom K, Chen G, Yu Q, Brage C, Rosen C. Promoted reactivity of char in co-gasification of
633 biomass and coal: synergies in the thermochemical process. *Fuel*. 1999(78):1189 - 94.
- 634 [23] Chen W-H, Wu J-S. An evaluation on rice husks and pulverized coal blends using a drop tube
635 furnace and a thermogravimetric analyzer for application to a blast furnace. *Energy*.
636 2009;34(10):1458-66.
- 637 [24] BS BS. *Solid Biofuels. Sample Preparation*. UK: BS; 2011.
- 638 [25] ISO IOFS. *Coal. Preparation of test samples Switzerland: ISO*; 2014.
- 639 [26] Yan J, Shi K, Pang C, Lester E, Wu T. Influence of minerals on the thermal processing of bamboo
640 with a suite of carbonaceous materials. *Fuel*. 2016;180:256-62.
- 641 [27] Parvez AM, Wu T. Characteristics and interactions between coal and carbonaceous wastes during
642 co-combustion. *Journal of the Energy Institute*. 2015.
- 643 [28] Jayaraman K, Gökalp I. Pyrolysis, combustion and gasification characteristics of miscanthus and
644 sewage sludge. *Energy Conversion and Management*. 2015;89:83-91.
- 645 [29] Pang CH, Gaddipatt S, Tucker G, Lester E, Wu T. Relationship between Thermal Behaviour of
646 Lignocellulosic Components and Properties of Biomass. *Bioresource Technology*. 2014;172:312-20.

647 [30] Celaya AM, Lade AT, Goldfarb JL. Co-combustion of brewer's spent grains and Illinois No. 6 coal:
648 Impact of blend ratio on pyrolysis and oxidation behavior. *Fuel Processing Technology*. 2015;129:39-
649 51.

650 [31] Wang J, Zhang S-y, Guo X, Dong A-x, Chen C, Xiong S-w, et al. Thermal Behaviors and Kinetics of
651 Pingshuo Coal/Biomass Blends during Copyrolysis and Cocombustion. *Energy & Fuels*.
652 2012;26(12):7120-6.

653 [32] Gil MV, Casal D, Pevida C, Pis JJ, Rubiera F. Thermal behaviour and kinetics of coal/biomass blends
654 during co-combustion. *Bioresource Technology*. 2010;101(14):5601-8.

655 [33] Shin S, Im SI, Kwon EH, Na J-G, Nho NS, Lee KB. Kinetic study on the nonisothermal pyrolysis of oil
656 sand bitumen and its maltene and asphaltene fractions. *Journal of Analytical and Applied Pyrolysis*.

657 [34] Song Z, Zhao X, Ma C, Wang T, Li L. Kinetics of Pyrolysis of Straw Bales by Microwave Heating.
658 Conference Kinetics of Pyrolysis of Straw Bales by Microwave Heating. p. 1-5.

659 [35] Rollinson AN, Karmakar MK. On the reactivity of various biomass species with CO₂ using a
660 standardised methodology for fixed-bed gasification. *Chemical Engineering Science*. 2015;128:82-91.

661 [36] Oladejo JM, Adegbite S, Pang CH, Liu H, Parvez AM, Wu T. A novel index for the study of synergistic
662 effects during the co-processing of coal and biomass. *Applied Energy*. 2017;188:215-25.

663 [37] Le Brech Y, Ghislain T, Leclerc S, Bouroukba M, Delmotte L, Brosse N, et al. Effect of Potassium on
664 the Mechanisms of Biomass Pyrolysis Studied using Complementary Analytical Techniques.
665 *ChemSusChem*. 2016;9(8):863-72.

666 [38] Grote K-H, Antonsson EK. *Springer Handbook of Mechanical Engineering*. New York: Springer
667 Science & Business Media, 2009.

668 [39] Ross AB, Jones JM, Cbaiklangmuang S, Pourkashanian M, Williams A, Kubica K, et al. Measurement
669 and Prediction of the Emissions of Pollutants from the Combustion in a Fixed Bed Furnace. *Fuel*.
670 2002;81:571 - 852.

671 [40] Vamvuka D, Salpigidou N, Kastanaki E, Sfakiotakis S. Possibility of using paper sludge in co-firing
672 applications. *Fuel*. 2009;88(2009).

673 [41] Blesa MJ, Miranda JL, Moliner R, Izquierdo MT, Palacios JM. Low-temperature co-pyrolysis of a
674 low-rank coal and biomass to prepare smokeless fuel briquettes. *Journal of Analytical and Applied
675 Pyrolysis* 2003;70:665–77.

676 [42] Idris SS, Rahman NA, Ismail K, Alias AB, Rashid ZA, Aris MJ. Investigation on thermochemical
677 behaviour of low rank Malaysian coal, oil palm biomass and their blends during pyrolysis via
678 thermogravimetric analysis (TGA). *Bioresource Technology* 2010;101:4584 - 92.

679 [43] Park DK, Kim SD, Lee SH, Lee JG. Co-pyrolysis characteristics of sawdust and coal blend in TGA and
680 a fixed bed reactor. *Bioresource Technology* 2010;101:6151-6.

681 [44] Tchapda AH, Pisupati SV. A Review of Thermal Co-Conversion of Coal and Biomass/Waste.
682 *Energies*. 2014;7:1098-148.

683 [45] Abbas T, Costen P, Kandamby NH, Lockwood FC, Ou JJ. The influence of burner injection mode on
684 pulverized coal and biosolid co-fired flames. *Combustion Flame*. 1994(99):617–25.

685 [46] Andries J, Verloop M, Hein K. Co-combustion of coal and biomass in a pressurized bubbling
686 fluidized bed. Conference Co-combustion of coal and biomass in a pressurized bubbling fluidized bed.,
687 Vancouver, Canada vol. 1. 14th International Conference on Fluidized Bed Combustion,, p. 313-20.

688 [47] Yorulmaz SY, Atimtay AT. Investigation of combustion kinetics of treated Fueland untreated waste
689 wood samples with thermogravimetric analysis. *Fuel Processing Technology*. 2009;90:939 - 46.

690 [48] Van Lith SC, Jensen PA, Frandsen FJ, Glarborg P. Release to the Gas Phase of Inorganic Elements
691 during Wood Combustion. Part 2: Influence of Fuel Composition. *Energy & Fuels* 2008;22(3): 1598-609

692 [49] Mason PE, Darvell LI, Jones JM, Williams A. Observations on the release of gas-phase potassium
693 during the combustion of single particles of biomass. *Fuel*. 2016;182:110-7.

694 [50] Wang K, Zhang J, Shanks BH, Brown RC. The deleterious effect of inorganic salts on hydrocarbon
695 yields from catalytic pyrolysis of lignocellulosic biomass and its mitigation. *Applied Energy*.
696 2015;148:115-20.

697 [51] Chen G, Yu Q, Brage C, Sjostrom K. Co-Gasification of Birch Wood and Daw Mill Coal in Pressurized
698 Fluidized Bed Gasifier: The Investigation into the Synergies in the Process. Conference Co-Gasification
699 of Birch Wood and Daw Mill Coal in Pressurized Fluidized Bed Gasifier: The Investigation into the
700 Synergies in the Process, Sevilla, Spain, . p. 1545 - 8.
701 [52] McKee DW, Spiro CL, Kosky PG, Lamby EJ. Catalysis of coal char gasification by alkali metal salts.
702 Fuel. 1983;62(2):217-20.
703 [53] Cheng S, Wei L, Zhao X, Julson J. Application, Deactivation, and Regeneration of Heterogeneous
704 Catalysts in Bio-Oil Upgrading. Catalysts. 2016;6(12):195.

705